Chapter 37
A Simple Qualitative Model for the Pressure-induced Expansion and Wall-stress Response of Fluid-filled Biological Channels

Tarek I. Zohdi

Abstract This work investigates the effects of a pressure increase in deformable fluid-filled biochannels, such as arteries and veins. Simple qualitative expressions are developed relating pressure-induced changes to the biochannel expansion, volumetric flow rate, and biochannel wall stress. Such relations are necessary for a rapid analysis in potential applications such as post-traumatic stress, hemorrhagic strokes, atherosclerotic plaque buildup, etc. The relations are based on the development of functions that correct classical pressurized thin-tube expressions for hoop stress for finite deformations.

Keywords: Pressure increase · Biochannels · Fluid flow

37.1 Introduction

This work studies the pressure-induced expansion and stress increase in deformable fluid-filled biochannels, such as arteries, vein, etc. This is motivated by interest in hypertension, hemorrhagic strokes and recently wide-spread interest in the effects of body-blows to pressure-induced biochannel rupture, arising from contact sports, such as boxing, football, ice-hockey, etc. Simple expressions are developed relating the pressure-induced changes to the biochannel expansion, volumetric flow rate and biochannel wall stress. Intended applications include post-traumatic stress, hemorrhagic strokes, atherosclerotic plaque buildup. The expressions developed allow for rapid analysis of such systems, circumventing the use of computationally-intensive numerical methods for detailed studies. The long-term objective is to couple such models to kinematic systems developed in Zohdi (2017) to simulate a wide range

Tarek I. Zohdi
Department of Mechanical Engineering, 6195 Etcheverry Hall, University of California, Berkeley, CA, 94720-1740, USA
e-mail: zohdi@berkeley.edu

B. E. Abali et al. (eds.), *New Achievements in Continuum Mechanics and Thermodynamics*, Advanced Structured Materials 108,
https://doi.org/10.1007/978-3-030-13307-8_37

of induced forces involving fist-to-head and fist-to-chest force calculations in order to determine the connections to possible channel expansion and wall-stress, leading to arterial rupture [1]. However, in certain circumstances, the fluid-induced shear stress may decrease, which increases the tendency of atherosclerotic plaque buildup (Zohdi, 2005, 2004, 2014). These scenarios are discussed further in the paper.

37.2 Classical Pressure-flow Relations

We consider a relatively simple model problem comprised of a biochannel which is filled with a fluid (such as blood, Fig. 37.1). By following Coleman et al (2012, Sect. 13.i), we consider a steady helical flow; by taking an annular element and summing the pressure and shear forces in the axial x-direction, we obtain

$$-\frac{\partial P}{\partial x} + \frac{1}{r}\frac{\partial (r\tau)}{\partial r} = 0 \Rightarrow \frac{1}{r}\frac{\partial (r\tau)}{\partial r} = \frac{\partial P}{\partial x}, \tag{37.1}$$

where P is the pressure and τ is the shear stress (in physical coordinates). Under the assumption that the pressure gradient is constant along the radius, integrating yields

$$\tau = \frac{r}{2}\left(\frac{\partial P}{\partial x}\right) + \frac{C_1}{r} = \mu\frac{\partial v}{\partial r}, \tag{37.2}$$

where v denotes the velocity along the axial direction and μ is the (shear) viscosity of the filling fluid. Integrating again yields

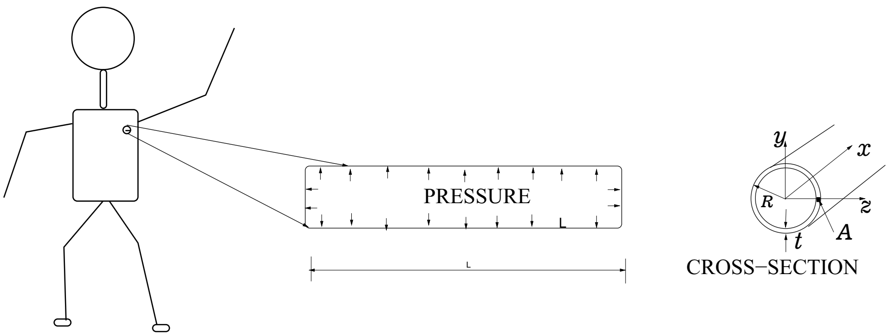

Fig. 37.1 Nomenclature for a simplified flow and stress analysis.

[1] This approach employs a combined kinematic and energy analysis, by drawing on methods used in the robotics literature (for example, see Hunt, 1978; Hartenberg and Denavit, 1964; Howell, 2001; McCarthy and Soh, 2010; McCarthy, 1990; Reuleaux, 1876; Sandor and Erdman, 1984; Slocum, 1992; Suh and Radcliffe, 1978; Uicker Jr et al, 2003).

$$v(r) = \frac{1}{\mu}\left(\frac{r^2}{4}\left(\frac{\partial P}{\partial x}\right) + C_1 \ln r\right) + C_2. \tag{37.3}$$

$v(r = 0)$ must be finite, thus $C_1 = 0$, and $v(r = R) = 0$ yields

$$v(r) = -\frac{R^2}{4\mu}\left(\frac{\partial P}{\partial x}\right)\left(1 - \left(\frac{r}{R}\right)^2\right). \tag{37.4}$$

The stress becomes

$$\tau(r) = \mu\frac{\partial v(r)}{\partial r} = \frac{r}{2}\frac{\partial P}{\partial x}. \tag{37.5}$$

The stress at the wall becomes

$$\tau_w = -\tau(r = R) = -\frac{R}{2}\frac{\partial P}{\partial x}. \tag{37.6}$$

An important observation is that if the radius of the channel grows, and the pressure gradient remains constant or grows, then the shear induced wall stress decreases. However, the flow rate can also be computed to reveal

$$\begin{aligned} Q = \int_A v\,dA = -\int_A \frac{R^2}{4\mu}\left(\frac{\partial P}{\partial x}\right)\left(1 - \left(\frac{r}{R}\right)^2\right) r dr d\theta = \\ = -\frac{2\pi R^2}{4\mu}\left(\frac{\partial P}{\partial x}\right)\left(\frac{r^2}{2} - \frac{r^4}{4R^2}\right)\Big|_{r=0}^{r=R} = -\frac{1}{\mu}\left(\frac{\partial P}{\partial x}\right)\frac{\pi R^4}{8}, \end{aligned} \tag{37.7}$$

thus indicating that decreasing R decreases the flow rate, if the pressure gradient does not increase appropriately. The implications of this are discussed further in the paper.

37.3 Simple Approximations of Radial Deformation

We now consider the radial deformation of the biochannel as a function of the pressure in the fluid (Fig. 37.1). We make the simplifying assumption that it is a thin-walled circular tube which expands self-similarly (uniformly) to a larger circular tube. At any point along the tube, the radial expansion is simplified by postulating it to be a linear function of the length-averaged mean pressure differential, $\Delta P^m = P^m - P_o^m$ with the nominal pressure P_o^m, of the form:

$$\frac{R}{R_o} = 1 + \mathcal{K}_w(P^m - P_o^m) = 1 + \mathcal{K}_w \Delta P^m, \tag{37.8}$$

where R is the deformed radius, R_o is the nominal (at $\Delta P^m = 0$) radius and $\mathcal{K}_w$ is a constant that represents the compliance of radial expansion. In order to determine the constant, consider a *thin-walled* cylindrical tube of mean radius R_o and thickness t_o is pressurized internally with ΔP^m. We also make the classical assumption that the tube is (eventually) closed at both ends. To calibrate/approximate the wall compliance constant, we can resort to its infinitesimal deformation response and we modify *the classical thin-walled tube approximations*, as explained next.

37.3.1 Estimate of Wall Stresses

We consider a tube with deformed radius R, thickness t and length L and initial radius R_o, thickness t_o and length L_o. For the thin-walled tube approximations, the stress components at point A in the wall (Fig. 37.1, far from the edges) of the tube, as a function of the applied pressure arise from the hoop (circumferential) stresses and the longitudinal stresses, leading to

$$[\boldsymbol{\sigma}] = \begin{bmatrix} \sigma_{xx} & \sigma_{xy} & \sigma_{xz} \\ \sigma_{yx} & \sigma_{yy} & \sigma_{yz} \\ \sigma_{zx} & \sigma_{zy} & \sigma_{zz} \end{bmatrix} = \begin{bmatrix} \Delta P^m R/2t & 0 & 0 \\ 0 & \Delta P^m R/t & 0 \\ 0 & 0 & 0 \end{bmatrix}. \tag{37.9}$$

37.3.2 Determination of the Compliance Constant

In order to calibrate the constant $\mathcal{K}_w$, we first assume a self-similar infinitesimal deformation, ignoring end-effects, with stresses given by

$$[\boldsymbol{\sigma}] = \begin{bmatrix} \sigma_{xx} & \sigma_{xy} & \sigma_{xz} \\ \sigma_{yx} & \sigma_{yy} & \sigma_{yz} \\ \sigma_{zx} & \sigma_{zy} & \sigma_{zz} \end{bmatrix} = \begin{bmatrix} \Delta P^m R_o/2t_o & 0 & 0 \\ 0 & \Delta P^m R_o/t_o & 0 \\ 0 & 0 & 0 \end{bmatrix}, \tag{37.10}$$

and linear elasticity, isotropic and homogeneous with Young's modulus E and Poisson ratio ν. The strains in the tube at point A can be computed to be, using Hooke's law:

$$\begin{aligned} [\boldsymbol{\epsilon}] &= \begin{bmatrix} \epsilon_{xx} & \epsilon_{xy} & \epsilon_{xz} \\ \epsilon_{yx} & \epsilon_{yy} & \epsilon_{yz} \\ \epsilon_{zx} & \epsilon_{zy} & \epsilon_{zz} \end{bmatrix} \\ &= \begin{bmatrix} \frac{\Delta P^m}{E}\frac{R_o}{t_o}(\frac{1}{2}-\nu) & 0 & 0 \\ 0 & \frac{\Delta P^m}{E}\frac{R_o}{t_o}(1-\frac{\nu}{2}) & 0 \\ 0 & 0 & -\frac{\Delta P^m}{E}\frac{R_o}{t_o}\frac{3\nu}{2} \end{bmatrix} \end{aligned} \tag{37.11}$$

The change in the tube radius

$$\Delta R/R_o = \frac{R-R_o}{R_o} \approx \epsilon_{yy},$$

by relating the perimeters:

$$2\pi R - 2\pi R_o \approx 2\pi R_o \epsilon_{yy} \Rightarrow \frac{R - R_o}{R_o} \approx \epsilon_{yy}. \tag{37.12}$$

Thus, one may immediately write

$$\frac{R - R_o}{R_o} = \frac{\Delta P^m}{E}\frac{R_o}{t_o}(1 - \frac{\nu}{2}) \Rightarrow R = R_o(1 + \frac{\Delta P^m}{E}\frac{R_o}{t_o}(1 - \frac{\nu}{2})) \tag{37.13}$$

Thus, an estimate of the compliance to radial expansion is

$$\mathcal{K}_w = \frac{R_o}{t_o E}(1 - \frac{\nu}{2}) \tag{37.14}$$

We assume that the wall compliance remains constant over the ΔP^m regimes of interest. At point A (the problem is radially symmetric), as a function of ΔP^m, the change in thickness is $\Delta t/t_o \approx \epsilon_{zz}$, which leads to

$$\frac{t - t_o}{t_o} = -\frac{\Delta P^m}{E}\frac{3\nu R_o}{2t_o} \Rightarrow t = t_o(1 - \frac{\Delta P^m}{E}\frac{3\nu R_o}{2t_o}). \tag{37.15}$$

37.3.3 Stress Correction Factors

For the finite deformation case, we approximate the stresses by

$$\sigma_{xx} = \frac{\Delta P^m R}{2t} \approx \frac{\Delta P^m R_o}{2t_o} \underbrace{\left[\frac{\left(1 + \frac{\Delta P^m}{E}\frac{R_o}{t_o}(1 - \frac{\nu}{2})\right)}{(1 - \frac{\Delta P^m}{E}\frac{3\nu R_o}{2t_o})}\right]}_{\text{correction factor} \stackrel{\text{def}}{=} \phi} = \frac{\Delta P^m R_o}{2t_o}\phi \tag{37.16}$$

and

$$\sigma_{yy} = \frac{\Delta P^m R}{t} \approx \frac{\Delta P^m R_o}{t_o}\left[\frac{(1 + \frac{\Delta P^m}{E}\frac{R_o}{t_o}(1 - \frac{\nu}{2}))}{(1 - \frac{\Delta P^m}{E}\frac{3\nu R_o}{2t_o})}\right] = \frac{\Delta P^m R_o}{t_o}\phi. \tag{37.17}$$

37.3.4 Corrected Material Failure Criteria

There are obviously many possible models for material failure. The most appropriate for a tubelike failure (longitudinal rupture) would likely be a hoop-stress failure criteria based on

$$\sigma_{yy} = \frac{\Delta P^m R}{t} \leq \sigma_H^* \tag{37.18}$$

so that

$$\frac{\Delta P^m R_o}{t_o} \leq \frac{\sigma_H^*}{\phi}, \tag{37.19}$$

where the correction factor ϕ by Eq. (37.16) is a function of ΔP^m. In order to isolate ΔP^m, we write inequality (37.19) by setting

$$A(\Delta P^m)^2 + B\Delta P^m + C = 0, \tag{37.20}$$

where

- $A = 1$,
- $B = \frac{t_o}{R_o c_2}\left(\frac{R_o}{t_o} + c_1\sigma_H^*\right)$, where $c_1 = \frac{R_o 3\nu}{2Et_o}$ and $c_2 = \frac{R_o}{Et_o}\left(1 - \frac{\nu}{2}\right)$ and
- $C = -\frac{\sigma_H^* t_o}{c_2 R_o}$.

Consequently, we have

$$\Delta P^m \leq \frac{1}{2A}\left(-B \pm \sqrt{B^2 - 4AC}\right) \tag{37.21}$$

which on taking the positive root leads to

$$\frac{R_o \Delta P^m}{t_o} \leq \frac{E\gamma}{2-\nu} \tag{37.22}$$

where γ is given by

$$\begin{aligned}\gamma &\stackrel{\text{def}}{=} -\left(1 + \frac{3\nu\sigma_H^*}{2E}\right) + \sqrt{\left(\left(1 + \frac{3\nu\sigma_H^*}{2E}\right)^2 + \frac{\sigma_H^* 2(2-\nu)}{E}\right)} = \\ &= -\left(1 + \frac{3\nu\sigma_H^*}{2E}\right) + \sqrt{1 + \frac{\sigma_H^*\nu}{E} + \frac{4\sigma_H^*}{E} + \left(\frac{3\nu\sigma_H^*}{2E}\right)^2}.\end{aligned} \tag{37.23}$$

We may then write

$$\frac{\Delta P^m R_o}{t_o} \leq \frac{E\gamma}{2-\nu} = \frac{E}{2-\nu}\left(-\left(1+\frac{3\nu\sigma_H^*}{2E}\right) + \right.$$
$$\left. +\sqrt{1+\frac{\sigma_H^*\nu}{E}+\frac{4\sigma_H^*}{E}+\left(\frac{3\nu\sigma_H^*}{2E}\right)^2}\,\right) \stackrel{\text{def}}{=} \sigma_H^{*,\text{corr}}, \tag{37.24}$$

which is a "corrected" failure criteria. We have a number of observations:

- **Observation** $\#1$**:** In special cases, such as $\nu = 0$ (no transverse contraction),

$$\gamma = -1 + \sqrt{\left(1+\frac{4\sigma_H^*}{E}\right)}, \tag{37.25}$$

thus

$$\frac{\Delta P^m R_o}{t_o} \leq \frac{E}{2}\gamma = \frac{E}{2}\left(\sqrt{1+\frac{4\sigma_H^*}{E}}-1\right). \tag{37.26}$$

One can linearize γ around $\sigma_H^* = 0$, yielding

$$\gamma = -1 + \sqrt{\left(1+\frac{4\sigma_H^*}{E}\right)} \approx \frac{2}{E}\sigma_H^*, \tag{37.27}$$

thus recovering

$$\frac{\Delta P^m R_o}{t_o} \leq \sigma_H^*, \tag{37.28}$$

for small values of σ_H^*.

- **Observation** $\#2$**:** The change in the domain length given by $\Delta L/L_o \approx \epsilon_{xx}$ tends to zero as the material becomes volume preserving, $\nu \to 1/2$, thus $L = L_0$. In this isochoric or incompressible case[2] of $\nu = \frac{1}{2}$ (incompressible)

$$\frac{\Delta P^m R_o}{t_o} \leq \frac{2E}{3}\left(-\left(1+\frac{3}{4}\frac{\sigma_H^*}{E}\right)+\sqrt{1+\frac{9\sigma_H^*}{2E}+\left(\frac{3\sigma_H^*}{4E}\right)^2}\right). \tag{37.29}$$

- **Observation** $\#3$**:** Although for soft tissue, a criterion based on von Mises equivalent stress would not be most appropriate, an estimate for the maximum allowable pressure, based on the von Mises (distortion energy) criterion is

$$\begin{aligned} 3||\boldsymbol{\sigma}'||^2 &= (\sigma_{xx}-\sigma_{yy})^2 + (\sigma_{xx}-\sigma_{zz})^2 + (\sigma_{yy}-\sigma_{zz})^2 + 6(\sigma_{xy}^2+\sigma_{xz}^2+\sigma_{yz}^2) \\ &= (\Delta P^m R/2t)^2 + (\Delta P^m R/2t)^2 + (\Delta P^m R/t)^2 + 6\tau_w^2 \\ &\leq 2\sigma_o^2, \end{aligned} \tag{37.30}$$

[2] Of course, an incompressible soft matter would be modeled by a hyperelastic material model stemming from energy description, herein we explain the physical significance by observing a volume preserving deformation.

where, σ_o is a material constant (failure stress) determined from a standard uniaxial failure tension test. There are, of course, numerous other criteria for failure.

37.4 Subsequent Flow Changes

Due the change in the radius, the fluid flow changes according to

$$\sigma_{xz} = \tau_w = -\frac{R}{2}\frac{\partial P}{\partial x} = -\frac{R_o}{2}\left(1 + \underbrace{\frac{\Delta P^m}{E}\frac{R_o}{t_o}\left(1 - \frac{\nu}{2}\right)}_{\lambda}\right)\frac{\partial P}{\partial x}, \tag{37.31}$$

where λ can be interpreted as a fluid-flow correction factor.

37.5 Closing Remarks

This work developed simple expressions between pressure change and mechanical response of the soft tissue filled with a fluid. The main results of the paper were, under some simplifying assumptions (self-similar expansion) at finite deformations:

- An expression relating the change in pressure
  - to the expansion of the biochannel radius,
  - to the reduction of the biochannel wall thickness,
  - to the wall stress of the biochannel,
- A flow correction relation for a biochannel with changing radius.

These relations are based on the development of functions that correct classical pressurized thin-tube expressions (ϕ) for hoop stress for finite deformations. Possible applications are to stroke and post-traumatic stress and, in particular, hemorrhagic strokes and alimentary rupture. The expressions developed allow for rapid analysis of such systems, reserving the direct use of computationally-intensive numerical methods for detailed studies as for example in Abali (2017). In closing, we make a few more observations with respect to flow changes and fluid-induced shear stresses, which were alluded to earlier in the paper. We note that $v(r)$ is a maximum where

$$\frac{\partial v}{\partial r} = 0 = \frac{r}{2\mu}\frac{\partial P}{\partial x}, \tag{37.32}$$

which is at $r = 0$. Thus,

$$v_{\max} = v(r=0) = -\frac{R^2}{4\mu}\left(\frac{\partial P}{\partial x}\right) \Rightarrow v(r) = v_{\max}\left(1 - \left(\frac{r}{R}\right)^2\right) \tag{37.33}$$

Relating this to the flow rate yields:

$$Q = \int_A v\, dA = \frac{\pi v_{\max} R^2}{2} \Rightarrow v_{\max} = \frac{2Q}{\pi R^2}, \tag{37.34}$$

and we obtain

$$v(r) = \frac{2Q}{\pi R^2}\left(1 - \left(\frac{r}{R}\right)^2\right) \tag{37.35}$$

The stress becomes

$$\tau(r) = \mu \frac{\partial v(r)}{\partial r} = -\frac{4\mu Q r}{\pi R^4}. \tag{37.36}$$

The stress at the wall becomes

$$\tau_w = -\tau(r = R) = \frac{2\mu v_{\max}}{R} = \frac{4\mu Q}{\pi R^3}. \tag{37.37}$$

Explicitly, the shear stress becomes:

$$\begin{aligned} \sigma_{xz} = \tau_w = -\frac{R}{2}\frac{\partial P}{\partial x} &= -\frac{R_o}{2}(1 + \frac{\Delta P^m}{E}\frac{R_o}{t_o}(1 - \frac{\nu}{2}))\frac{\partial P}{\partial x} = \frac{4\mu Q}{\pi R^3} \\ &= \frac{4\mu Q}{\pi\left(R_o(1 + \frac{\Delta P^m}{E}\frac{R_o}{t_o}(1 - \frac{\nu}{2}))\right)^3}. \end{aligned} \tag{37.38}$$

Thus, unless Q increases appropriately, the fluid-induced shear stress at the wall will decrease. For example, consider an increase in volumetric flow rate due to the change in lumen (cavity of the artery) diameter of the following form

$$Q(\Delta P) = \pi R^2 v^m, \tag{37.39}$$

where $R = R(\Delta P)$ and v^m (the mean velocity) is constant, which implies from Equation 37.7 that

$$v^m = -\frac{1}{\mu}\frac{\partial P}{\partial x}\frac{R^2}{8}, \tag{37.40}$$

which leads to

$$\tau_w = \frac{4\mu Q}{\pi R^3} = \frac{4\mu\pi R^2 v^m}{\pi R^3} = \frac{4\mu v^m}{R}. \tag{37.41}$$

Thus, the wall shear stress will decrease. Low wall shear stress is associated with the growth of plaque buildup (Zohdi, 2005, 2004, 2014; Zohdi et al, 2004), due to the accumulation of material in diseased arteries. This is often the initial stage of arterial occlusive growth processes (Ambrosi et al, 2011; Göktepe et al, 2010; Menzel and Kuhl, 2012; Kuhl et al, 2007; Zöllner et al, 2012). For surveys of plaque-related work, see Chyu and Shah (2001); Davies et al (1993); Corti et al (2002); Kaazempur-Mofrad et al (2005, 2004, 2003); Libby (2001); Libby et al (2001, 2002); Libby and Aikawa (2002); Loree et al (1992); Richardson et al (1989); Shah (1997); van der Wal and Becker (1999). Thus, in addition to coronary diseases, the accumulation of material subsequently reduces the cross-sectional area of the biochannel, which can lead to dementia-like symptoms, potentially due to the build up of calcium and fatty deposits on biochannel walls (Wenk et al, 2010; Klepach et al, 2012; Lee et al, 2013; Weinberg et al, 2009). This is under current investigation by the author.

References

Abali BE (2017) Computational Reality: Solving nonlinear and coupled problems in continuum mechanics. Springer Nature

Ambrosi D, Ateshian G, Arruda E, Cowin S, Dumais J, Goriely A, Holzapfel GA, Humphrey JD, Kemkemer R, Kuhl E, et al (2011) Perspectives on biological growth and remodeling. Journal of the Mechanics and Physics of Solids 59(4):863–883

Chyu KY, Shah PK (2001) The role of inflammation in plaque disruption and thrombosis. Reviews in cardiovascular medicine 2(2):82–91

Coleman BD, Markovitz H, Noll W (2012) Viscometric flows of non-Newtonian fluids: theory and experiment, vol 5. Springer Science & Business Media

Corti R, Badimon L, Fuster V, Badimon J (2002) Assessing and modifying the vulnerable atherosclerotic plaque, chapter endothelium, flow, and artherothrombosis. American Heart Association

Davies MJ, Richardson PD, Woolf N, Katz DR, Mann J (1993) Risk of thrombosis in human atherosclerotic plaques: role of extracellular lipid, macrophage, and smooth muscle cell content. Heart 69(5):377–381

Göktepe S, Abilez OJ, Parker KK, Kuhl E (2010) A multiscale model for eccentric and concentric cardiac growth through sarcomerogenesis. Journal of theoretical biology 265(3):433–442

Hartenberg R, Denavit J (1964) Kinematic Synthesis of Linkages, McGraw-Hill Book Company. McGraw-Hill, New York

Howell LL (2001) Compliant mechanisms. John Wiley & Sons

Hunt KH (1978) Kinematic geometry of mechanisms, vol 7. Oxford University Press, USA

Kaazempur-Mofrad M, Younis H, Patel S, Isasi A, Chung C, Chan R, Hinton D, Lee R, Kamm R (2003) Cyclic strain in human carotid bifurcation and its potential correlation to atherogenesis: Idealized and anatomically-realistic models. Journal of Engineering Mathematics 47(3-4):299–314

Kaazempur-Mofrad M, Isasi A, Younis H, Chan R, Hinton D, Sukhova G, LaMuraglia G, Lee R, Kamm R (2004) Characterization of the atherosclerotic carotid bifurcation using mri, finite element modeling, and histology. Annals of biomedical engineering 32(7):932–946

Kaazempur-Mofrad M, Wada S, Myers J, Ethier C (2005) Blood flow and mass transfer in arteries with axisymmetric and asymmetric stenoses. Int J Heat Mass Transfer 48:4510–4517

Klepach D, Lee LC, Wenk JF, Ratcliffe MB, Zohdi TI, Navia JL, Kassab GS, Kuhl E, Guccione JM (2012) Growth and remodeling of the left ventricle: a case study of myocardial infarction and surgical ventricular restoration. Mechanics research communications 42:134–141

Kuhl E, Maas R, Himpel G, Menzel A (2007) Computational modeling of arterial wall growth. Biomechanics and modeling in mechanobiology 6(5):321–331

Lee LC, Wenk JF, Zhong L, Klepach D, Zhang Z, Ge L, Ratcliffe MB, Zohdi TI, Hsu E, Navia JL, et al (2013) Analysis of patient-specific surgical ventricular restoration: importance of an ellipsoidal left ventricular geometry for diastolic and systolic function. Journal of applied physiology 115(1):136–144

Libby P (2001) Current concepts of the pathogenesis of the acute coronary syndromes. Circulation 104(3):365–372

Libby P, Aikawa M (2002) Stabilization of atherosclerotic plaques: new mechanisms and clinical targets. Nature medicine 8(11):1257–1262

Libby P, Ridker PM, Maseri A (2002) Inflammation and atherosclerosis. Circulation 105(9):1135–1143

Libby P, et al (2001) The vascular biology of atherosclerosis (ed. E. Braunwald and D. P. Zipes and P. Libby), vol Chap. 30. Saunders, Philadelphia, Pennsylvania

Loree HM, Kamm RD, Stringfellow RG, Lee RT (1992) Effects of fibrous cap thickness on peak circumferential stress in model atherosclerotic vessels. Circulation research 71(4):850–858

McCarthy JM (1990) Introduction to theoretical kinematics. MIT press

McCarthy JM, Soh GS (2010) Geometric design of linkages, vol 11. Springer Science & Business Media

Menzel A, Kuhl E (2012) Frontiers in growth and remodeling. Mechanics research communications 42:1–14

Reuleaux F (1876) Book Review: The Kinematics of Machinery (trans. and annotated by A. B. W. Kennedy). reprinted by Dover, New York (1963)

Richardson PD, Davies M, Born G (1989) Influence of plaque configuration and stress distribution on fissuring of coronary atherosclerotic plaques. The Lancet 334(8669):941–944

Sandor GN, Erdman AG (1984) Mechanism design: analysis and synthesis, vol 1. Prentice-Hall New Delhi

Shah PK (1997) Plaque disruption and coronary thrombosis: new insight into pathogenesis and prevention. Clinical cardiology 20(11 Suppl 2):II–38

Slocum AH (1992) Precision machine design. Society of Manufacturing Engineers

Suh C, Radcliffe C (1978) Kinematics and mechanisms design. john willey & sons. New York

Uicker Jr J, Pennock G, Shigley J (2003) Theory of mechanisms and machines

van der Wal AC, Becker AE (1999) Atherosclerotic plaque rupture–pathologic basis of plaque stability and instability. Cardiovascular research 41(2):334–344

Weinberg EJ, Schoen FJ, Mofrad MR (2009) A computational model of aging and calcification in the aortic heart valve. PLoS One 4(6):e5960

Wenk JF, Papadopoulos P, Zohdi TI (2010) Numerical modeling of stress in stenotic arteries with microcalcifications: a micromechanical approximation. Journal of biomechanical engineering 132(9):091,011

Zohdi T (2004) A computational framework for agglomeration in thermochemically reacting granular flows. Proceedings of the Royal Society of London A: Mathematical, Physical and Engineering Sciences 460(2052):3421–3445

Zohdi T (2005) A simple model for shear stress mediated lumen reduction in blood vessels. Biomechanics and modeling in mechanobiology 4(1):57–61

Zohdi T (2014) Mechanically driven accumulation of microscale material at coupled solid–fluid interfaces in biological channels. Journal of The Royal Society Interface 11(91):20130,922

Zohdi T (2017) On the biomechanical analysis of the calories expended in a straight boxing jab. Journal of The Royal Society Interface 14(129):20170,153

Zohdi T, Holzapfel G, Berger S (2004) A phenomenological model for atherosclerotic plaque growth and rupture. Journal of theoretical biology 227(3):437–443

Zöllner AM, Tepole AB, Kuhl E (2012) On the biomechanics and mechanobiology of growing skin. Journal of theoretical biology 297:166–175